

# Continuum of ground states and aperiodic structures in a lattice gas on the triangular lattice with finite-range interactions

Yu. I. Dublenych

*Institute for Condensed Matter Physics, National Academy of Sciences of Ukraine, 1 Svientsitskii Street, 79011 Lviv, Ukraine*

(Received 2 February 2012; revised manuscript received 29 April 2012; published 5 July 2012)

A continuum of ground states is shown to exist in a lattice-gas model with one particle species on a triangular lattice with finite-range interactions. The structures of the continuum can be divided into three groups: periodic (up to phason flips along some channels), multiple-twin, and aperiodic. We suppose that there are quasicrystalline structures among the latter. The growth mechanism for the structures consists in continuous formation and self-destruction of defects through the propagation of phasonic excitations. Our investigation sheds light on some fundamental questions in the theory of quasicrystals and infinitely adaptive structures.

DOI: [10.1103/PhysRevB.86.014201](https://doi.org/10.1103/PhysRevB.86.014201)

PACS number(s): 61.44.Br, 68.43.Fg, 64.75.Yz, 89.75.Kd

## I. INTRODUCTION

The problem of structure or pattern formation is among the most important and interesting problems in modern physics. However, in spite of several decades of intensive studies in this field, many fundamental key questions still remain unanswered, in particular, the following ones. Why are quasicrystals—ordered but aperiodic structures with the point spectrum whose indexing requires a number of vectors that is finite but greater than dimensionality of the structures—formed and how do they grow?<sup>1,2</sup> What is the mechanism of infinite adaptivity in some compounds where, “within certain composition limits, every composition can attain a fully ordered crystal structure”?<sup>3–6</sup> Do ordered structures which are neither conventional crystals nor quasicrystals (for example the so-called almost periodic crystals<sup>7</sup> and irregularly ordered structures)<sup>8</sup> exist? We hope that our investigation reported here and subsequent studies will shed some light on all these problems.

We consider a rather simple lattice-gas model with one particle species on a triangular lattice with finite-range interactions and we show that this model possesses a continuum of ground states parameterized with the particle density or even (if the interaction reaches eighth neighbors) with the chemical potential. The continuum contains both periodic (up to phason flips along some channels) and aperiodic structures. It is quite probable that there are quasicrystals as well as non-quasicrystalline aperiodic structures among the latter.

So far, there is no general agreement regarding the role of energy and entropy in the stability of quasicrystals.<sup>9–11</sup> Energy stabilization presupposes the existence of perfect quasicrystalline ground states. If, on the contrary, the role of entropy is predominant, then quasicrystals can exist only for sufficiently high temperatures and turn into periodic crystals as temperature decreases. Our results support the energetic concept of stabilization for aperiodic structures (including quasicrystalline ones).



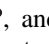

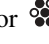
The description of quasicrystalline structures is based on the mathematical theory of aperiodic tilings. This kind of tiling was considered as long ago as 1619 by Kepler.<sup>12</sup> Nowadays, an aperiodic tiling was obtained for the first time by Berger in 1964.<sup>13</sup> It was constructed with the so-called Wang dominoes. As to lattice-gas models with aperiodic ground states, they appeared in 1980s<sup>14</sup> (immediately after the discovery of

quasicrystals).<sup>15</sup> However, all these models are based on some aperiodic tilings and contain many particle species (at least 16). We have managed to obtain aperiodic structures in a lattice model with one particle species only.

Up to now, it is not clear how quasicrystals grow. Mathematical matching rules in the theory of tiling lead to the nonlocality of growth. This fact had suggested that these rules are not physical because they require long-range interactions to form perfect quasicrystalline structures. Subsequently, it has been shown that perfect Penrose tilings can be obtained using a local growth algorithm which corresponds to short-range interactions.<sup>16,17</sup> The model to be considered in this paper contains only finite-range interactions while the growth mechanism for aperiodic and even periodic structures is nonlocal. This mechanism can be called “phasonic” since it assumes that the defects, inevitable in the growth process, destruct themselves due to successive phason flips of particles.

The existence of the ground-state continuum in the model considered here proves that infinite adaptivity observed in many compounds<sup>3</sup> can occur in systems with finite-range interactions. This contradicts the Kittel’s suggestion that infinite adaptivity is due to the long-range interactions.<sup>4</sup> Let us note that some numerical results corroborate with the Kittel’s suggestion,<sup>5</sup> but in Ref. 6 the infinite adaptivity was obtained, numerically as well, in a system with finite-range interactions. Our results are all the more significant since they are analytical and cannot be obtained numerically.

## II. CONTINUUM OF GROUND STATES

Thus, let us consider a lattice gas with one particle species on a triangular lattice. In Ref. 18 we have proved that, in the five-dimensional parameter space which includes pairwise interactions of first, second, and third neighbors, three-particle nearest-neighbor interaction, and the chemical potential, a four-dimensional polyhedral cone (4-face of a five-dimensional region) exists where the ground-state structures of the corresponding lattice-gas model are constructed with the following set of configurations of the “flower” (a site with six neighboring sites): , , , and  (or ). This means that each flower in these structures belongs to some of these four types. In what follows, we have to consider the interactions up to eighth neighbors. Therefore, instead of the

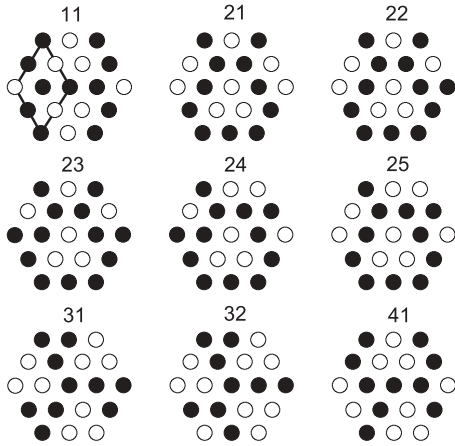


FIG. 1. The set of big-flower configurations equivalent to the set  $\text{⬢⬢⬢⬢}$ ,  $\text{⬢⬢⬢⬢}$ ,  $\text{⬢⬢⬢⬢}$ , and  $\text{⬢⬢⬢⬢}$ . Solid circles represent particles and open ones represent vacancies.

set of flower configurations we will have to use an equivalent set of configurations of a bigger cluster containing 19 sites (Fig. 1). We call this cluster “big flower.” For the sake of convenience, we enumerate the configurations of the big flower by two indexes, the first of which is the number of the small flower in the center of the big one.

Each site on the triangular lattice is the center of a big flower. We refer to the relative number of a big-flower configuration in a structure as the “fractional content” of this configuration in the structure. In addition to the trivial relation between fractional contents  $k_{ij}$  of the nine big-flower configurations in the structures generated, some other linear relations hold. A general method to deduce them is described in Ref. 19.

Let us consider a diamondlike subcluster of the big flower. This subcluster can occupy two nonequivalent positions in the big flower: central (position 1) and lateral (position 2). Each big diamond on the lattice belongs to one big flower in the central position ( $c_1 = 1$ ) and to two big flowers in lateral positions ( $c_2 = 2$ ). Let us consider a big-diamond configuration, for instance, the one shown in Fig. 1, and calculate the numbers  $n_{1,ij}$  and  $n_{2,ij}$  of diamonds with this configuration in each big-flower configuration in the positions 1 and 2, respectively:  $n_{1,32} = 1$ ,  $n_{2,11} = 2$ ,  $n_{2,22} = 1$ ,  $n_{1,23} = 2$ . All the remaining numbers  $n_{i,ij}$  are equal to zero. Using the general relation

$$\sum_{ij} \frac{k_{ij} n_{1,ij}}{c_1} = \sum_{ij} \frac{k_{ij} n_{2,ij}}{c_2}, \quad (1)$$

we get

$$k_{32} = \frac{2k_{11} + k_{22} + 2k_{23}}{2}. \quad (2)$$

Having considered other diamond configurations, one obtains six linear relations (in addition to the trivial one) between fractional contents  $k_{ij}$  of nine big-flower configurations in the structures that they generate:

$$\begin{aligned} k_{32} &= 2k_{11}, \\ 2k_{21} + k_{22} &= 2k_{11}, \\ k_{25} + k_{32} &= 2k_{32}, \\ 2k_{25} + 2k_{24} &= 2k_{41}, \\ 3k_{31} + k_{32} + k_{41} &= 2k_{41}, \\ 2k_{11} + k_{22} + 2k_{23} &= 2k_{32}, \\ k_{11} + k_{21} + k_{22} + k_{23} + k_{24} + k_{25} + k_{31} + k_{32} + k_{41} &= 1. \end{aligned} \quad (3)$$

From these relations we have

$$\begin{aligned} k_{11} &= \frac{3 - 7k_4}{13}, \quad k_{22} = -2k_{21} + \frac{6 - 14k_4}{13}, \quad k_{23} = k_{21}, \\ k_{24} &= \frac{-6 + 27k_4}{13}, \quad k_{25} = \frac{6 - 14k_4}{13}, \quad k_{31} = \frac{-2 + 9k_4}{13}, \\ k_{32} &= \frac{6 - 14k_4}{13}, \end{aligned} \quad (4)$$

where  $k_4 = k_{41}$  is the fractional content of the configuration  $\text{⬢⬢⬢⬢}$  in the structure.

Since we consider many-particle couplings we set a distinction of site clusters and particle clusters (i.e., occupied-site clusters). To avoid confusion, we call the latter “filled clusters” or briefly “f-clusters.” Consider an f-cluster  $\mathbf{K}$  and the corresponding coupling. To calculate the energy density of a structure, it is necessary to know the density of f-clusters  $\mathbf{K}$  in this structure, that is, the number of f-clusters  $\mathbf{K}$  per site. The simplest f-cluster is a single particle, and the corresponding density  $p_0$  is the number of particles *per site*. Instead of the number of f-clusters  $\mathbf{K}$  per site, we use the number  $p_{\mathbf{K}}$  of f-clusters  $\mathbf{K}$  *per particle*. The density of f-clusters  $\mathbf{K}$  is equal to  $p_0 p_{\mathbf{K}}$ , where

$$p_{\mathbf{K}} = \frac{1}{c_{\mathbf{K}} p_0} \sum a_{ij} k_{ij}. \quad (5)$$

Here  $c_{\mathbf{K}}$  is the number of big flowers on the lattice which contain a cluster  $\mathbf{K}$ ;  $a_{ij}$  is the number of f-clusters  $\mathbf{K}$  in the corresponding big-flower configuration. The sum runs over all big-flower configurations depicted in Fig. 1.

Let us find  $p_i$  ( $i = 0 - 8$ ) and  $p_{\Delta}$ , where  $p_0$  is the number of particles per site (i.e., density of particles or coverage),  $p_i$  ( $i = 1 - 8$ ) provides the number of  $i$ th neighbor pairs of particles per particle (two-particle f-clusters), and  $p_{\Delta}$  is the number of triplets of nearest-neighbor particles per particle (three-particle f-cluster):

$$\begin{aligned} p_0 &= \frac{1}{19} (11k_1 + 11k_{21} + 12k_{22} + 13k_{23} + 12k_{24} + 11k_{25} + 10k_{31} + 9k_{32} + 10k_4) = \frac{7 + k_4}{13}, \\ p_{\Delta} &= \frac{1}{12p_0} (k_{22} + 2k_{23} + 2k_{24} + k_{25} + 3k_{31} + k_{32} + k_4) = \frac{13}{3} - \frac{7}{3p_0}, \quad p_1 = 5 - \frac{2}{p_0}, \quad p_2 = -2 + \frac{2}{p_0}, \quad p_3 = 5 - \frac{2}{p_0}, \\ p_4 &= 8 - \frac{2}{p_0}, \quad p_5 = 12 - \frac{6}{p_0}, \quad p_6 = -2 + \frac{2}{p_0}, \quad p_7 = 10 - \frac{4}{p_0}, \quad p_8 = -16 + \frac{10 + k_{21}}{p_0}. \end{aligned} \quad (6)$$

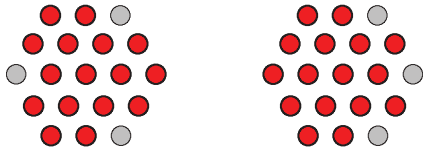



FIG. 2. (Color online) Maximal clusters (in red) on the triangular lattice with the diameter not greater than the distance between seventh neighbors.

Thus, we see that the densities  $p_0 p_i$  ( $i = 1-7$ ) and  $p_0 p_{\Delta}$  linearly depend on the particle density  $p_0$ . For eighth neighbors, this dependence is no longer linear. It is easy to prove that for any f-cluster  $\mathbf{K}$  with the diameter not greater than the distance between seventh neighbors, the  $p_0$  dependence of  $p_0 p_{\mathbf{K}}$  is linear. Such an f-cluster is an f-subcluster at least of one of the two maximal f-clusters with the diameter equal to the distance between seventh neighbors (Fig. 2). It is sufficient to prove that, for each f-subcluster  $\mathbf{K}$  of those maximal f-clusters, the following equality holds:

$$n_{21} + n_{23} = 2n_{22}, \quad (7)$$

where  $n_{21}$ ,  $n_{23}$ , and  $n_{22}$  are the numbers of f-subclusters  $\mathbf{K}$  in the big-flower configurations 21, 23, and 22, respectively. Then  $p_{\mathbf{K}}$  depends on  $k_4$  only (which, in turn, linearly depends on  $p_0$ ) and does not depend on  $k_{21}$ . Analyzing configurations 21, 23, and 22, one can easily see that this equality holds for all the f-subclusters of the maximal f-clusters depicted in Fig. 2.

Now, let us find the dependence of  $k_{21}$  on  $p_0$ . Consider all structures constructed with the set of big-flower configurations depicted in Fig. 1 (or with the equivalent set of flower configurations ) in such a manner that the big-flower configuration 31 is contained in each structure. One can show that such structures can be partitioned into domains

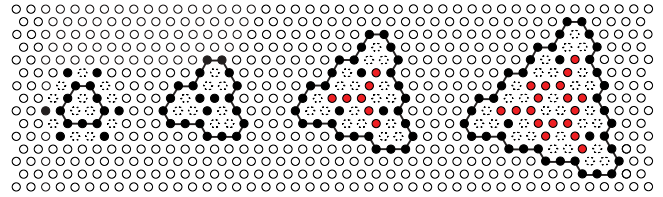


FIG. 3. (Color online) Hierarchy of domains with sides equal to 1, 2, 3, 4, ... zigzags. Occupied sites are depicted as black and red circles and unoccupied ones are depicted as open dotted circles.

whose hierarchy is depicted in Fig. 3, and only two or three consecutive members of the hierarchy can be contained in the same structure. The domains are joined six by six as shown in Fig. 4. Examples of structures and their domain schemes are presented in Fig. 5.

The domain, whose side is equal to  $k$  zigzags, has  $9k$  peripheral and  $(k-1)(2k-1)$  interior occupied sites; the number of unoccupied sites is equal to  $\frac{3k(k+1)}{2}$ . Each junction of six domains contains three sites common for three domains. Hence, there are  $\frac{3}{2}$  sites per domain which are common for three domains. The rest of peripheral sites are common for two domains. Therefore, the number of occupied sites which belong to the same domain with the side equal to  $k$ , is given by

$$2k^2 + \frac{3}{2}k + \frac{1}{4} = \frac{(2k+1)(4k+1)}{4}. \quad (8)$$

Let the side of the minimal domain in a structure be equal to  $k$  and the fractional content of these domains be equal to  $n_1$ . Let us denote the fractional contents of domains whose sides are equal to  $k + 1$  and  $k + 2$  by  $n_2$  and  $n_3$ , respectively. Then, a simple calculation yields an expression for the particle density in the corresponding structure, that is,

$$p_0 = \frac{(8k^2 + 6k + 1)n_1 + (8k^2 + 22k + 15)n_2 + (8k^2 + 38k + 45)n_3}{(14k^2 + 12k + 1)n_1 + (14k^2 + 40k + 27)n_2 + (14k^2 + 68k + 81)n_3}. \quad (9)$$

Configurations 21 occur uniquely at the junctions of six domains (see Fig. 4) and there are three of them at every junction. Hence, the fractional content of these configurations in a structure is given by

$$k_{21} = \frac{6}{(14k^2 + 12k + 1)n_1 + (14k^2 + 40k + 27)n_2 + (14k^2 + 68k + 81)n_3}. \quad (10)$$

Let us consider a structure with three types of domains. Such a structure can be partitioned into wide and narrow stripes. The narrow stripes are composed with little and middle domains and the wide stripes are composed with middle and big domains. This partition into parallel stripes is unique for a given structure and can be performed in three directions simultaneously. At the overlap of two narrow stripes, there are small and middle domains; at the overlap of two wide stripes there are middle and big domains; and at the overlap of narrow and wide stripes there are two middle domains. Two narrow or two big domains cannot occur at the overlap of any two stripes. If the structure is periodic and its period contains

$s$  narrow and  $l$  wide stripes, then a unit cell contains  $s^2$  small,  $l^2$  big, and  $s^2 + l^2 + 4sl$  middle domains. The fractional contents of small ( $n_1$ ), middle ( $n_2$ ), and big ( $n_3$ ) domains are given by

$$n_1 = \frac{s^2}{2(s+l)^2}, \quad n_2 = \frac{s^2 + 4sl + l^2}{2(s+l)^2}, \quad n_3 = \frac{l^2}{2(s+l)^2}. \quad (11)$$

These relations yield the following ones:

$$n_2 = \frac{1}{2} - 2n_1 + \sqrt{2n_1}, \quad n_3 = \frac{1}{2} + n_1 - \sqrt{2n_1}. \quad (12)$$

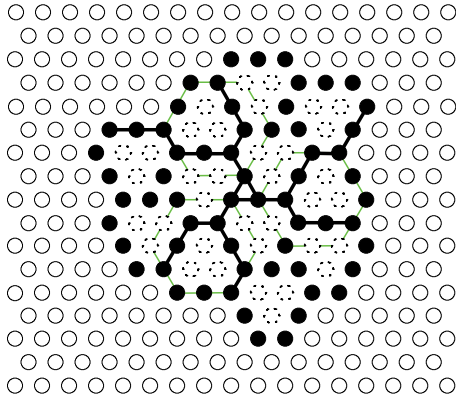
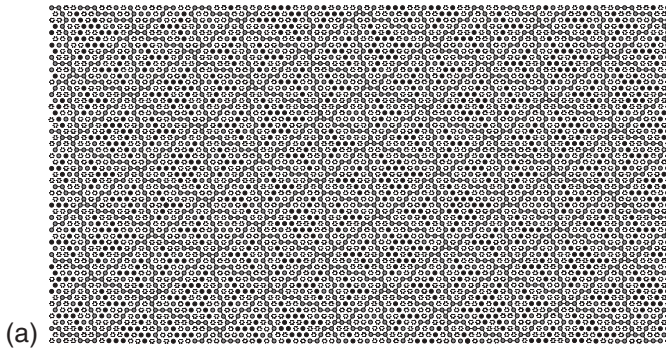


FIG. 4. (Color online) Junction of domains. Configurations 21 are shown by green hexagons.

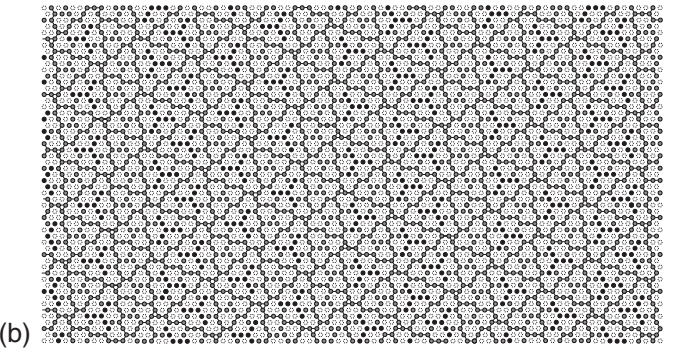
It is obvious that relations (11) and, hence, relations (12) hold for aperiodic structures and also for the structures with only two types of domains ( $n_3 = 0$ ).

One can observe and prove that the structures under consideration are completely determined by the system of trefoils (or configurations 31). Let us introduce the value  $r$ , which is the average distance between neighboring trefoils (the unit of the distance is the triplet of unoccupied sites surrounded by occupied ones). It can be shown that  $r$  is described by the expression

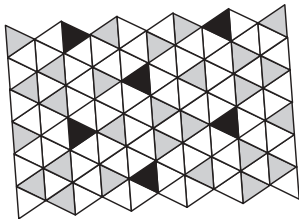
$$r = \frac{s + 2l + k(s + l)}{-s + k(s + l)} = \frac{2 + k - \sqrt{2n_1}}{k - \sqrt{2n_1}}. \quad (13)$$



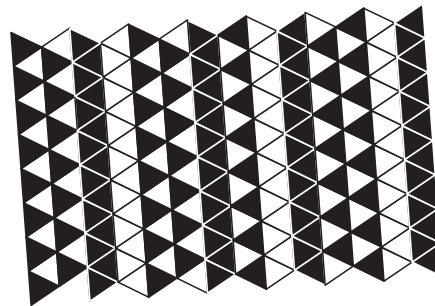
(a)



(b)



(c)



(d)

FIG. 5. Examples of structures generated by the set of configurations depicted in Fig. 1 with (a) three ( $p_0 = \frac{460}{823}$ ) and (b) two ( $p_0 = \frac{34}{61}$ ) types of domains. (c),(d) The schemes of their domain superstructures. Occupied sites are depicted as black and gray circles and unoccupied ones are depicted as open dotted circles. Small, middle, and big domains are represented by black, white, and gray triangles, respectively.

Now expressions (9) and (10) for  $p_0$  and  $k_{21}$  can be rewritten in a simpler form, that is,

$$p_0 = \frac{1 + 15r^2}{1 + 27r^2}, \quad k_{21} = \frac{3(r - 1)^2}{1 + 27r^2}. \quad (14)$$

Using these expressions, we can write  $k_{21}$  and, hence,  $p_8$  in terms of  $p_0$ . Thus, we have

$$k_{21} = \frac{13p_0 - 7 - \sqrt{3(1 - p_0)(9p_0 - 5)}}{2}, \quad (15)$$

$$p_8 = -\frac{19}{2} + \frac{13 - \sqrt{3(1 - p_0)(9p_0 - 5)}}{2p_0}. \quad (16)$$

These expressions are valid for  $\frac{5}{9} < p_0 \leq \frac{4}{7}$ , that is, for the structures containing configurations 31. Now we have to consider the structures without configuration 31. These have been partially analyzed in Ref. 18 (structures 12). For these structures  $p_0 = \frac{5}{9}$ ,  $k_4 = \frac{2}{9}$ , and  $k_{21}$  varies from  $\frac{1}{9}$  [structure 12a, Fig. 6(b)] to  $\frac{2}{27}$  [structure 12b, Fig. 6(c)].

Let  $I_1$ ,  $I_2$ ,  $I_3$ , and  $I_8$  be the first-, second-, third-, and eighth-neighbor couplings, respectively, and let  $I_\Delta$  be the three-body coupling. We do not consider interactions corresponding to other f-subclusters of maximal f-clusters because their densities depend on  $p_0$  linearly and, therefore, the corresponding couplings do not shift the degeneracy in the boundary under consideration. This degeneracy is shifted by the interaction of eighth neighbors. The energy of structure(s)



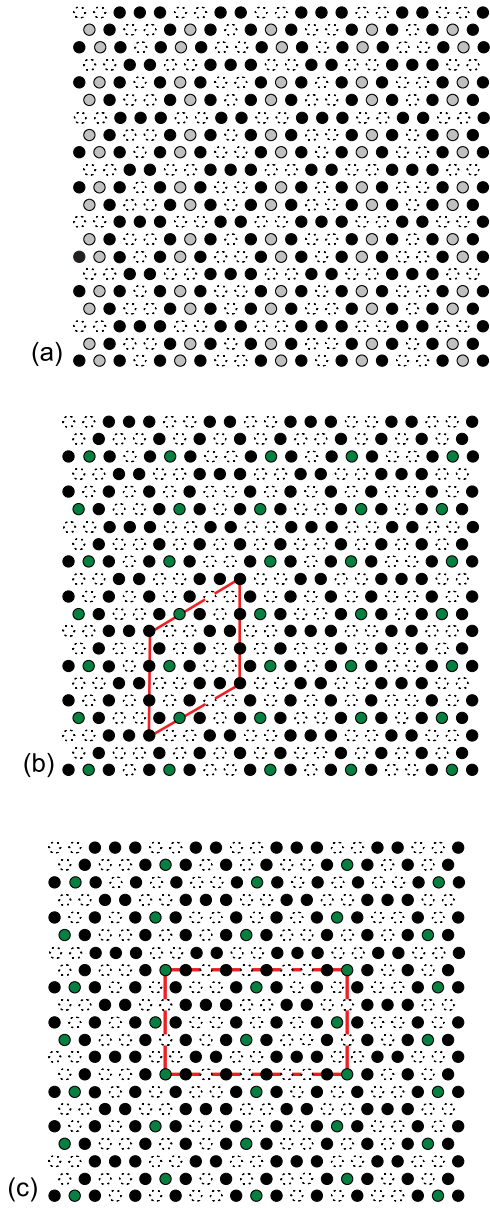


FIG. 6. (Color online) (a) Structures 12. In every zigzag, either upper or lower gray circles in each pair should be solid (but identically for each pair of the zigzag). (b) Structure 12a with the smallest unit cell. (c) Structure 12b.

with particle density  $p_0$  is given by

$$E = p_0(p_1 I_1 + p_2 I_2 + p_3 I_3 + p_8 I_8 + p_\Delta I_\Delta - \mu_{lg}). \quad (17)$$

Having made use of the expressions (6) for  $p_1$ ,  $p_2$ ,  $p_3$ ,  $p_8$ , and  $p_\Delta$ , we obtain

$$E = p_0 \left( 5I_1 - 2I_2 + 5I_3 + \frac{13}{3}I_\Delta - \mu_{lg} - \frac{19}{2}I_8 \right) - \frac{\sqrt{3(1-p_0)(9p_0-5)}}{2} I_8 - \left( 2I_1 - 2I_2 + 2I_3 + \frac{7}{3}I_\Delta - \frac{13}{2}I_8 \right). \quad (18)$$

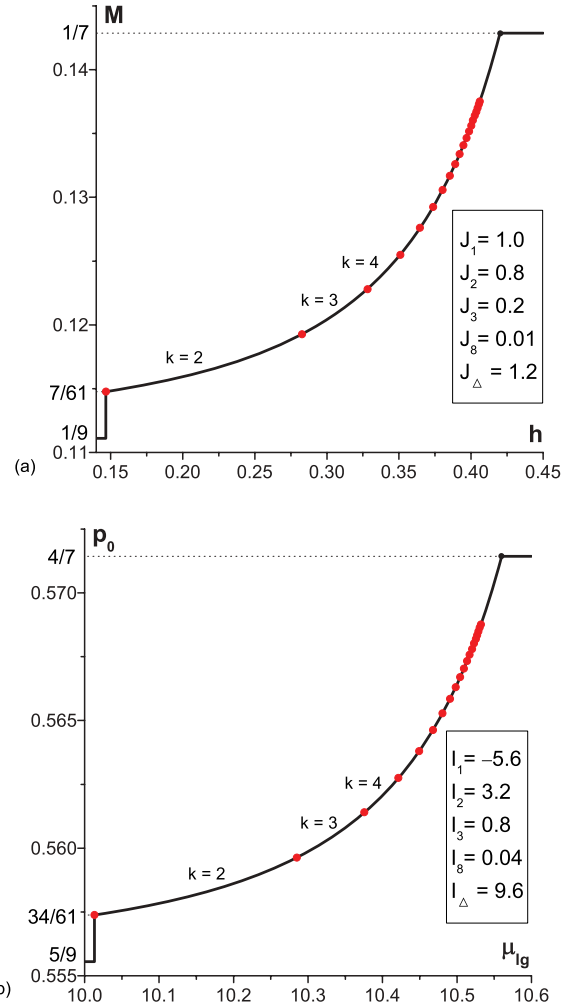


FIG. 7. (Color online) (a) Dependence of magnetization on the external field and (b) dependence of the density of particles on the chemical potential in the region with the continuum of ground states. The first 20 points which correspond to the structures with two types of domains are shown. The particle densities for these points are  $p_0 = \frac{4k^2+7k+4}{7k^2+13k+7}$  ( $k = 2, 3, \dots$  is the dimension of the small domain in zigzags).

The equation for the hyperplane in which the ground state is the structure(s) with particle density  $p_0$  is given by

$$\frac{\partial E}{\partial p_0} = 0, \quad \frac{\partial^2 E}{\partial p_0^2} > 0, \quad (19)$$

or, in the explicit form,

$$5I_1 - 2I_2 + 5I_3 + \frac{13}{3}I_\Delta - \mu_{lg} - \frac{19}{2}I_8 + \frac{3(9p_0-7)}{2\sqrt{3(1-p_0)(9p_0-5)}} I_8 = 0, \quad I_8 > 0. \quad (20)$$

We should verify, however, whether any of the structures 12 have smaller energies on this hyperplane. Since  $I_8 > 0$ , structure 12b has the minimal energy among all the structures 12. This energy is given by

$$E_{12b} = \frac{5}{9} \left( \frac{7}{3}I_1 + \frac{8}{3}I_2 + \frac{7}{3}I_3 + \frac{32}{15}I_8 + \frac{2}{15}I_\Delta - \mu_{lg} \right). \quad (21)$$

After having equated energies (18) and (21), and taking into account Eq. (20), we find that these energies are equal for  $p_0 = \frac{34}{61}$ . The relevant hyperplane is described by the equation

$$5I_1 - 2I_2 + 5I_3 + \frac{13}{3}I_\Delta - \frac{89}{3}I_8 - \mu_{lg} = 0. \quad (22)$$

Hence, for the particle density in the interval from  $\frac{34}{61}$  to  $\frac{4}{7}$ , we have a continuum of ground states; that is, there is a one-to-one correspondence between the values of particle densities from this interval and the hyperplanes in the Hamiltonian parameter space.

We can easily switch to the equivalent spin model with spin variables  $\sigma = \pm 1$ , using the transformation of the interaction parameters that is given by (see Ref. 18)

$$\begin{aligned} I_1 &= 4J_1 - 8J_\Delta, \quad I_i = 4J_i \quad (i = 2, 3, 8), \quad I_\Delta = 8J_\Delta, \\ \mu_{lg} &= 2h + 12(J_1 + J_2 + J_3 + J_8 - J_\Delta), \quad p_0 = \frac{1+M}{2}, \end{aligned} \quad (23)$$

where  $M$  is magnetization per site. For the spin model, Eq. (20) is substituted with

$$\begin{aligned} 4J_1 - 10J_2 + 4J_3 + \frac{10}{3}J_\Delta - h - 25J_8 \\ + \frac{3(9M - 5)}{\sqrt{3(1 - M)(9M - 1)}}J_8 = 0, \end{aligned} \quad (24)$$

The continuum of ground states exists for the magnetization in the interval from  $\frac{7}{61}$  to  $\frac{1}{7}$ . The dependence of magnetization on the external field in this interval is shown in Fig. 7(a). The corresponding dependence of the particle density on the chemical potential is shown in Fig. 7(b). We suppose that  $J_8 = 0.01$  is small enough not to go out of the region with the continuum of ground states.

As is clear from Fig. 7, the phase transition from phase 12 to the phase with  $p_0 = \frac{34}{61}$  is a first-order transition and the transition from the continuum of ground states to the limiting phase with  $p_0 = \frac{4}{7}$  (Fig. 8) is a continuous one.

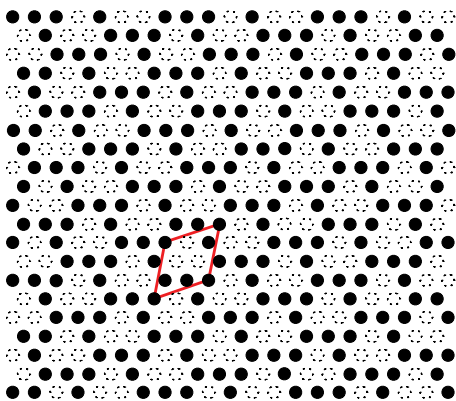


FIG. 8. (Color online) The limiting structure of the continuum of ground states ( $p_0 = \frac{4}{7}$ ). It is constructed with flower configurations  $\text{⬢⬢⬢}$ ,  $\text{⬢⬢⬢⬢}$ , and  $\text{⬢⬢⬢⬢⬢}$ .

### III. STRUCTURES OF THE CONTINUUM AND THE MECHANISM OF THEIR GROWTH

#### A. Fractional content of small domains in a narrow stripe of a structure as its determining characteristic

Now, let us analyze the structures in themselves. We call the scheme of domains of a structure (see Fig. 5) its “1-structure.” The structure itself will be called “0-structure.” First we consider the structures with three types of domains. Let  $c_1$  be the fractional content of small domains in a narrow stripe of a structure. It is easy to see that this value is the same for all narrow stripes in the structure irrespective of their orientations and that it is equal to

$$c_1 = \frac{s}{2(s+l)} = \frac{k}{2} + \frac{1}{1-r}, \quad 0 < c_1 < \frac{1}{2}. \quad (25)$$

The fractional content (relative number) of big domains in a wide stripe is given by

$$C_1 = \frac{1}{2} - c_1. \quad (26)$$

The average distance between trefoils can be expressed in terms of  $c_1$  or  $C_1$ :

$$r = \frac{2}{k - 2c_1} + 1 = \frac{2}{k + 2C_1 - 1} + 1. \quad (27)$$

The fractional contents of small and big domains are also related to  $c_1$  and  $C_1$ , respectively,

$$\begin{aligned} n_1 &= \frac{1}{2} \left( k - \frac{2}{r-1} \right)^2 = 2c_1^2, \\ n_3 &= \frac{1}{2} \left( k - \frac{r+1}{r-1} \right)^2 = 2C_1^2. \end{aligned} \quad (28)$$

The particle density is a function of  $c_1$  and  $k$ , that is,

$$p_0 = \frac{4(2c_1 - k)^2 - 15(2c_1 - k - 1)}{7(2c_1 - k)^2 - 27(2c_1 - k - 1)}. \quad (29)$$

In order to construct a 1-structure(s) with fixed  $c_1$ , one has to start with only one stripe of black and white triangles (“narrow” or “black” stripe), its density of black triangles being equal to  $c_1$ , or with a stripe of white and gray triangles (“wide” or “gray” stripe), its density of gray triangles being equal to  $C_1 = \frac{1}{2} - c_1$ . However, these stripes cannot be arbitrary. They should be compatible with the rule for construction of 1-structures (which was already formulated above): At the overlap of two narrow, two wide, and narrow and wide stripes, there should be black and white, white and gray, and two white triangles, respectively. This rule determines the stripe, which is, for instance, the left neighbor to the constructed one, either uniquely or in two ways. Some examples of 1-structures are shown in Fig. 9. If the sides of all black and gray triangles from two neighboring stripes lie in their midline, then these two stripes can be reflected with respect to their midline. We call such a line a “disorder line” or a “phasonic line.” For the 1-structure with the density of black triangles equal to  $c_1 = \frac{p}{q}$  ( $p$  and  $q$  are relative primes), the distance between consecutive phasonic lines is equal to  $q$  triangles if  $q$  is even and to  $2q$  triangles if  $q$  is odd. Hence, all structures with rational  $c_1$  are disordered. There occurs ordering along the direction of the phasonic lines and disorder in other two directions. Therefore,

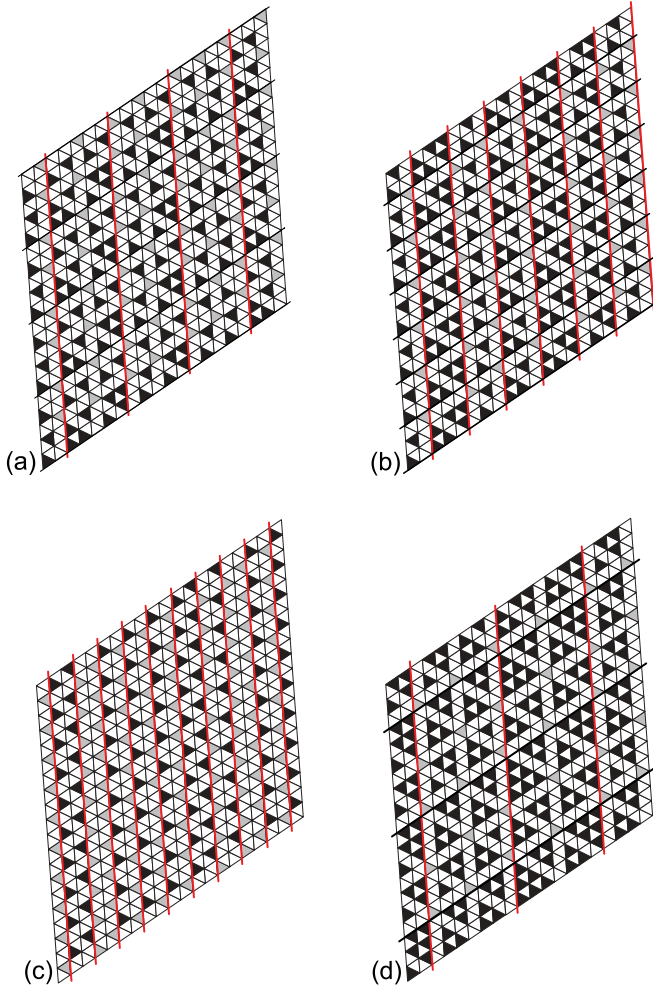


FIG. 9. (Color online) 1-structures with (a)  $c_1 = \frac{3}{10}$ , (b)  $c_1 = \frac{1}{3}$ , (c)  $c_1 = \frac{1}{4}$ , and (d)  $c_1 = \frac{5}{14}$ . Black, white, and gray triangles represent small, middle, and big domains, respectively. The vertical red lines are the phasonic lines (see text). The black heavy lines reflect the periodicity in the vertical direction. 1-structure (c) is 2-structure of 0-structures with 1-structure (d).

this disorder can be called one-dimensional; it does not lead to residual entropy. The disorder is due to phason flips that do not change the energy density of structures. We can single out the periodic 1-structure with the smallest unit cell from the infinite number of 1-structures corresponding to a rational  $c_1$ . The choice of the unit cell for this 1-structure is not unique. The uniqueness can be ensured by the following condition: Two consecutive phasonic lines should contain two parallel sides of the unit cell while black triangles with their sides on a vertical phasonic line should lie to its right (see Fig. 10).

In what follows, we write simply “1-structure with  $c_1$ ” using the expression “1-structure with the density of black triangles equal to  $c_1$ .”

### B. Transformations of structures

1-structures are connected to one another by some transformations and thus we may restrict their analysis to a part of 1-structures only. Let us consider some of these transformations.

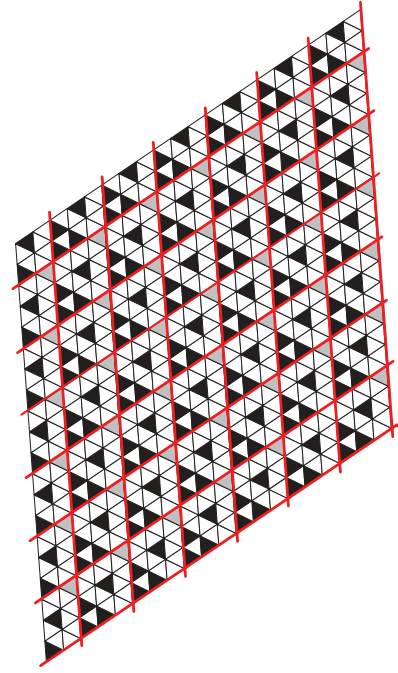


FIG. 10. (Color online) The periodic 1-structure with  $c_1 = \frac{1}{3}$  and the smallest unit cell. Black, white, and gray triangles represent small, middle, and big domains, respectively.

In a 1-structure with  $c_1$ , black triangles can be replaced with gray ones and vice versa. Then we obtain a 1-structure with  $\tilde{c}_1 = \frac{1}{2} - c_1$ . The invariant of this transformation is the 1-structure with  $c_1 = \frac{1}{4}$  [Fig. 9(c)]. Therefore, it is sufficient to consider the 1-structures with  $\frac{1}{4} \leq c_1 \leq \frac{1}{2}$ , that is, the 1-structures where the density of gray triangles does not exceed the density of black ones. In this interval, function  $p_0(k, c_1)$  decreases. For  $k = 2$ , the value  $p_0$  varies from  $\frac{34}{61}$  ( $c_1 = \frac{1}{2}$ ) to  $\frac{62}{111}$  ( $c_1 = \frac{1}{4}$ ).

Let us consider one more transformation of 1-structures. As one can see from Fig. 9, the black triangles in 1-structures with  $\frac{1}{4} \leq c_1 \leq \frac{1}{2}$  are organized in triangular domains. The maximum number of different domains is three again: small, middle, and big ones, exactly as the domains in 0-structures. The unique 1-structure with only one type of “black” domains (as well as “gray” ones) is the 1-structure with  $c_1 = \frac{1}{4}$ . We call these new domains “1-domains” and the scheme thereof is called “2-structure” (certainly, with respect to the 0-structure). It is clear that 2-structures are at the same time 1-structures for corresponding 0-structures. Here is an example: The 1-structure with  $c_1 = \frac{1}{3}$  [Fig. 9(b)] is a 2-structure for the 0-structure with  $c_1 = \frac{7}{20}$  [Fig. 11(a)].

The fractional content  $c_2$  of small 2-domains in each narrow stripe of a 2-structure is related to the fractional content  $c_1$  of small 1-domains in each narrow stripe of the 1-structure as given by

$$c_2 = 1 + \frac{k_1}{2} - \frac{c_1}{1 - 2c_1}, \quad (30)$$

where  $k_1$  is a side of the small 1-domain. The inverse of this relation is

$$c_1 = \frac{1}{2} \left( 1 - \frac{1}{k_1 + 3 - 2c_2} \right). \quad (31)$$

Using this transformation (in the general case, more than one time), we can transform each 1-structure with three types of domains into a 1-structure with one or two types of domains only.

In what follows, we refer to a stripe composed of elementary triangles (black and white or gray and white) as a “row” and we consider stripes consisting of rows. If, in a 1-structure with  $c_1 = \frac{1}{4}$ , all one-row black stripes are replaced with two-row ones, then we obtain a 1-structure with  $c_1 = \frac{1}{3}$ . The 1-structures with  $\frac{1}{4} < c_1 < \frac{1}{3}$  contain both one- and two-row black stripes. If all one-row black stripes in such a 1-structure are replaced with two-row ones and vice versa, then we obtain a 1-structure with

$$\tilde{c}_1 = \frac{3 - 8c_1}{4(2 - 5c_1)}. \quad (32)$$

The invariant of this transformation is a 1-structure with  $c_1 = \frac{3}{10}$  [Fig. 9(a)], where the numbers of one-row and two-row black stripes are equal.

If  $m$  one-row stripes are inserted (in all the three directions) between each pair of consecutive two-row stripes (there can be some one-row stripes between them yet) in a 1-structure with  $\frac{1}{4} < c_1 < \frac{1}{3}$ , then we obtain a 1-structure with

$$c_{1m} = \frac{m(4c_1 - 1) + 2c_1}{2[2m(4c_1 - 1) + 1]}. \quad (33)$$

Negative  $m$  corresponds to the decrease of the number of one-row stripes between successive pairs of two-row stripes. The 1-structures with  $\frac{3}{10} \leq c_1 < \frac{1}{3}$  contain pairs of two-row stripes without one-row stripes between them.

If, in a 1-structure with  $\frac{1}{4} < c_1 < \frac{1}{3}$ ,  $m$  two-row stripes are inserted (in all three directions) between each pair of consecutive one-row stripes (there can be some two-row stripes between them yet), then we obtain a 1-structure with

$$c_{1m} = \frac{2m(3c_1 - 1) - c_1}{6m(3c_1 - 1) - 1}. \quad (34)$$

Negative  $m$  corresponds to the decrease of the number of two-row stripes between successive pairs of one-row stripes. The 1-structures with  $\frac{1}{4} \leq c_1 < \frac{5}{16}$  contain pairs of one-row stripes without two-row stripes between them.

As follows from the above reasoning, 1-structures with  $\frac{3}{10} \leq c_1 < \frac{5}{16}$  contain pairs of one-row stripes with no two-row stripes between them as well as pairs of two-row stripes with no one-row stripes between them. It is sufficient to consider only these 1-structures.

It should be noted that the sides of all the 1-domains in 1-structures can be increased equally (new 1-domains with the sides equal to 1 can appear in this case). It is easy to prove that the increase of the sides of all the 1-domains by  $m$  (negative  $m$  corresponds to the decrease) leads to the 1-structure with

$$c_{1m} = \frac{m(2c_1 - 1) - 2c_1}{2[m(2c_1 - 1) - 1]}. \quad (35)$$

An example of such 1-structures is shown in Fig. 11.

### C. Construction of a black stripe with the use of the Farey tree

How to construct a black stripe compatible with the rule of structure construction? It is clear that there is an infinite number of such stripes. Let us consider black stripes parallel

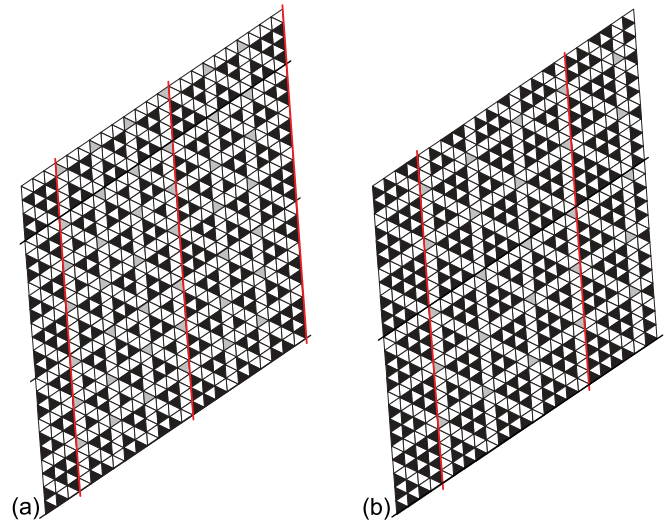


FIG. 11. (Color online) 1-structures with (a)  $c_1 = \frac{7}{20}$  and (b)  $c_1 = \frac{5}{13}$ . Black, white, and gray triangles represent small, middle, and big domains, respectively. The vertical red lines are the phasonic lines (see text). The black heavy lines reflect the periodicity in the vertical direction.

to the phasonic lines. The black stripe which is adjacent to a phasonic line can be singled out. We have not found any simple algorithm to construct this stripe. However, it turns out that each 1-structure contains a black stripe (parallel to the phasonic lines) which can be constructed with the use of the Farey tree, that is, a binary tree of rational numbers between 0 and 1. The Farey tree has been used to construct the ground states of the lattice gas models mostly in one dimension, but also in two dimensions (see Ref. 20 and references therein). The left part of the Farey tree is shown in Fig. 12. The tree extends downward to infinity according to the following rule: Each pair of adjacent fractions  $\frac{p_1}{q_1}$  and  $\frac{p_2}{q_2}$  has the descendant  $\frac{p_1 + p_2}{q_1 + q_2}$ . Every rational number between 0 and 1 occurs once in the tree. The stripe with  $c_1 = \frac{p}{q}$  has the period of  $q$  triangles if  $q$  is an even number and this period is a concatenation of the periods of two fractions parent for the fraction  $\frac{p}{q}$  in the Farey tree. If  $q$  is odd, then the period is equal to  $2q$  triangles. One white and one black triangle (marked as “−” and “+”) are the periods for  $\frac{0}{1}$  and  $\frac{1}{1}$ , respectively. If  $c_1$  is an irrational number, then we construct an infinite sequence of rational numbers which lead to  $c_1$  along the branches of the Farey tree. (One can say that irrational numbers are located

